KERNFORSCHUNGSANLAGE JÜLICH GmbH
Institut für Plasmaphysik
Association EURATOM-KFA

Measurement of Electron Densities and Temperatures in the Plasma Boundary Combining Neutral Beam Probes and Laser-induced Fluorescence

by

K. Kadota, A. Pospieszczyk, P. Bogen, E. Hintz

Jül - 1812
Oktober 1982
ISSN 0366-0885

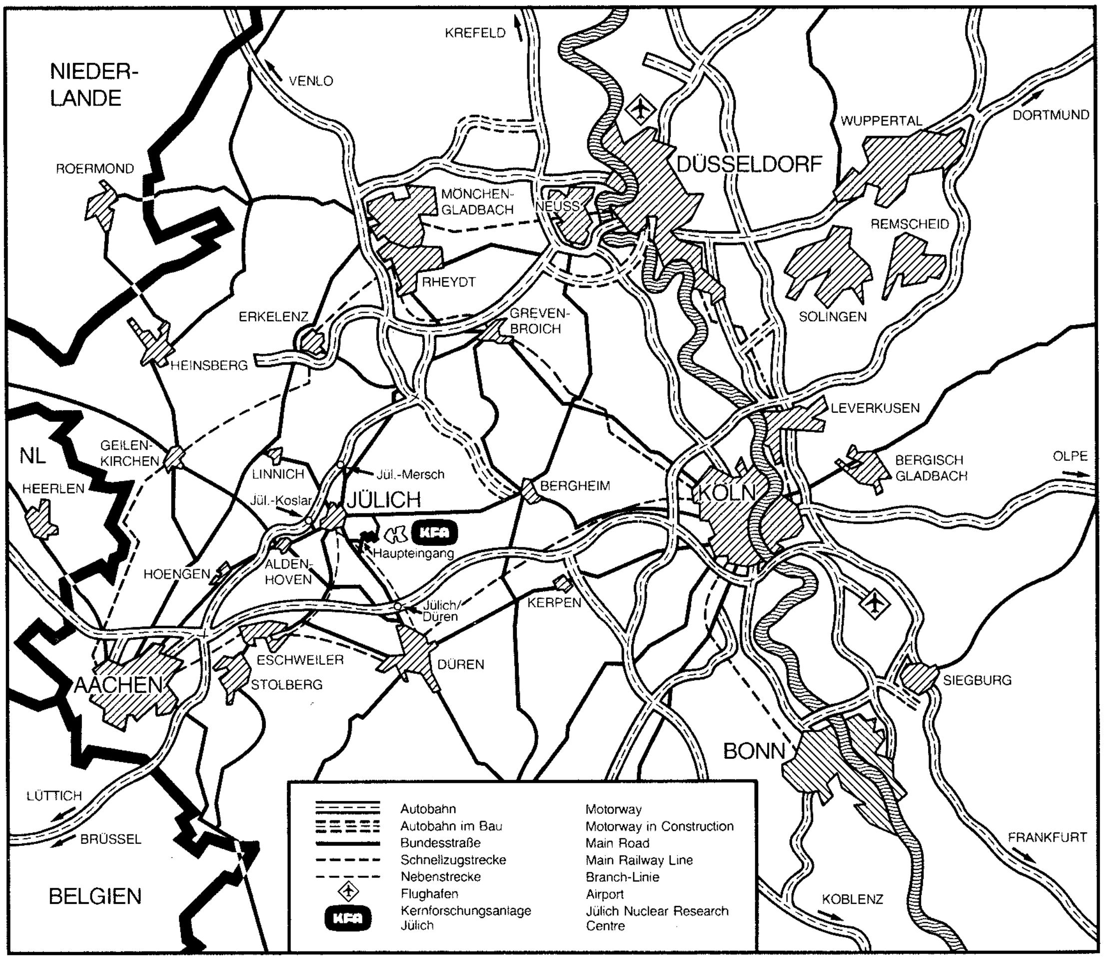

Als Manuskript gedruckt

Berichte der Kernforschungsanlage Jülich – Nr. 1812
Institut für Plasmaphysik Association EURATOM-KFA Jül - 1812

Zu beziehen durch: ZENTRALBIBLIOTHEK der Kernforschungsanlage Jülich GmbH
Postfach 1913 · D-5170 Jülich (Bundesrepublik Deutschland)
Telefon: 02461/610 · Telex: 833556 kfa d

Measurement of Electron Densities and Temperatures in the Plasma Boundary Combining Neutral Beam Probes and Laser-induced Fluorescence

by

K. Kadota, A. Pospieszczyk, P. Bogen, E. Hintz

Measurement of Electron Densities and Temperatures in the Plasma Boundary Combining Neutral Beam Probes and Laser-induced Fluorescence

K. Kadota+), A. Pospieszczyk, P. Bogen and E. Hintz
Institut für Plasmaphysik der Kernforschungsanlage Jülich GmbH,
Association EURATOM-KFA, 517o Jülich, F R G

Abstract

A new diagnostic method using both techniques of neutral beam probing and laser-induced fluorescence (LIF) is proposed to measure electron density (10^{11} - 10^{13} cm^{-3}) and electron temperature (1 - 100 eV) of a boundary layer plasma in devices like tokamaks. The local electron density can be obtained by measuring the photon flux of the resonance line produced by electron impact excitation of an injected neutral Li-beam which is produced by laser-induced evaporation (LIE). The density of the neutral Li-beam which is necessary for the determination of the electron density is measured by LIF. The local electron temperature can be obtained by determining the attenuation of two neutral beams (Li, and Al or Ti) produced by LIE, of which the measurements are carried out by means of LIF. The applicability of this method to the TEXTOR tokamak is discussed in detail.

+) Permanent address: Institute of Plasma Physics, Nagoya University, Nagoya, Japan

1. Introduction

Controlled thermonuclear fusion research has been remarkably progressed, as tokamaks take a leading part in it. One of the problems to be solved in order to operate tokamaks as a fusion reactor is the protection of the first wall from the large power loading and the control of impurities originating from the plasma-wall-interaction.

Plasma parameters in the boundary layer are very important for investigations related to this problem. So far, Langmuir probes have mainly been used for this purpose. The insertion of such probes into a plasma, however, causes serious disturbances to the plasma. For instance, the impurity transport is not yet completely understood due to poor information of the impurity behaviour in the boundary layer, of which one reason is the inaccurate knowledge of the plasma parameters.

Neutral Li-beam probes at energies from thermal (attenuation method) to several keV (emission method) have been developed and applied to measure electron density profiles of Nagoya Bumpy Torus (NBT) in which n_e is of the order of 10^{11} cm^{-3} /1,2/. Energetic neutral metal beams (0.1 eV - 10 eV) produced by laser-induced evaporation (LIE) have been developed for the study of impurity behaviour in tokamaks /3,4,5/.

The laser-induced fluorescence (LIF) technique has been used to measure the density and the velocity distribution of metal atoms, the purpose of which is the study of the plasma-wall-interaction in fusion research devices /6,7/. This technique was applied to measure e.g. the density of Ti atoms in the ASDEX tokamak /8/ and Al atoms in Elmo Bumpy Torus (EBT) /9/. During the course of these experiments, the electron temperature was estimated by measuring the attenuation of the sputtered atoms. The combined technique of LIE and LIF has been used to investigate the diffusion of Al atoms in plasmas /1o/.

In this paper we propose a new method of measuring electron density (10^{11} - 10^{13} cm^{-3}) and electron temperature (1 - 100 eV) of plasmas in the boundary layer by means of the combined technique of slow neutral beam probes (1 - 10 eV beams produced by LIE) and LIF.

The principle of this method is described in section 2. The requirements for its application to the boundary layer plasmas are given in sections 3 and 4. The accuracy of it and its applicability to the TEXTOR tokamak is discussed in sections 5 and 6, repectively.

2. Principle of the Method

2.1 Measurement of electron density

In the boundary layer, the dominant attenuation process of a metal-atom beam, A, injected at an energy below 1 keV is electron impact ionization,

$$A + e \rightarrow A^{+} + 2e. \qquad (1)$$

The differential attenuation of the atomic beam is given by the following formula,

$$\frac{1}{I_A(x)} \frac{dI_A(x)}{dx} = -n_e(x) \frac{\langle \sigma_i^A v \rangle}{v_A} = -n_e(x)\, f_A(T_e(x)), \qquad (2)$$

where $I_A(x)$ is the local beam intensity, $\langle \sigma_i^A v \rangle / v_A$ the effective cross section for process (1) which is only a function of T_e, and v_A the beam velocity. If a species like alkali atoms for which $\langle \sigma_i^A v \rangle / v_A$ is insensitive to T_e is used, we can obtain the local electron density $n_e(x)$ or the electron line density $\int n_e(x)dx$ from the beam attenuation /2/. A method for its measurement is proposed below.

When the energetic metal atoms, A, are injected into a plasma, they emit photons by electron impact excitation,

$$A + e \rightarrow A^{*} + e \rightarrow A + e + h\nu \;. \qquad (3)$$

The locally emitted photon flux $N_\nu^{ex}(x)$, is given by the following formula,

$$N_\nu^{ex}(x) = n_A(x)\, n_e(x)\, \langle \sigma_{ex} v \rangle\, V_b, \qquad (4)$$

where $n_A(x)$ is the local atom density, $n_e(x)$ the local electron density, $\langle \sigma_{ex} v \rangle$ the rate coefficient for process (3) which is a function of electron temperature T_e, and V_b the observation volume determined by the diameter of the probing atomic beam.

The local atom density $n_A(x)$ can be obtained by means of LIF,

$$A + h\nu \rightarrow A^* \rightarrow A + h\nu' \quad (\nu' \leq \nu), \qquad (5)$$

where the case of $\nu' = \nu$ corresponds to the two level system.
We consider the two level case in order to simplify the discussion.
In the saturation condition, the flux , $N_\nu^{fl}(x)$, of photons emitted by process (5) is given by the following formula,

$$N_\nu^{fl}(x) = \frac{g_2}{g_1 + g_2} n_A(x) \quad A_{21} \quad V_1, \qquad (6)$$

where g_1 and g_2 are the statistical weights of the related lower and upper levels, respectively, A_{21} the transition probability and V_1 the observation volume determined by the diameter of the pumping laser beam.

From formulae(4) and (6) the following formula can be derived,

$$n_e(x) = \frac{g_2}{g_1 + g_2} \frac{A_{21}}{\langle \sigma_{ex} v \rangle} \frac{V_1}{V_b} \frac{N_\nu^{ex}(x)}{N_\nu^{fl}(x)} . \qquad (7)$$

If A_{21} and $\langle \sigma_{ex} v \rangle$ are known and $\langle \sigma_{ex} v \rangle$ is insensitive to T_e, we can obtain the local electron density $n_e(x)$ from the measurement of the ratio of the local photon fluxes, $N_\nu^{ex}(x)/N_\nu^{fl}(x)$, as the ratio V_1/V_b is determined by the geometry.

2.2 Measurement of Electron Temperature

If in the measurement of the differential beam attenuation $n_e(x)$ is known, we can determine the value of $\langle \sigma_i^A v \rangle / v_A$ from formula 2 and then obtain the local electron temperature $T_e(x)$ by using an atomic beam for which the effective cross section for electron impact ionization is sensitive to T_e /8,9/. The accuracy of this method, however, is limited by that of $n_e(x)$ in addition to that of the ionization cross section.
When the attenuation of another atomic beam, B, is measured in addition to that of the atomic beam, A,

$$\frac{1}{I_B(x)} \frac{dI_B(x)}{dx} = -n_e(x) \frac{\langle \sigma_i^B v \rangle}{v_B} = -n_e f_B(T_e(x)), \qquad (8)$$

the demerit above can be overcome and $T_e(x)$ can be obtained without the knowlege of $n_e(x)$. From formulae (2) and (8), we obtain the following formula,

$$\frac{\frac{1}{I_A(x)} \frac{dI_A(x)}{dx}}{\frac{1}{I_B(x)} \frac{dI_B(x)}{dx}} = \frac{\frac{\langle \sigma_i^A v \rangle}{v_A}}{\frac{\langle \sigma_i^B v \rangle}{v_B}} = \frac{f_A(T_e(x))}{f_B(T_e(x))} = g(T_e(x)). \qquad (9)$$

Since the left hand side of formula (9) can be represented by the term of the photon flux produced by LIF,

$$N_\nu^{fl}(x) = C \frac{I_b(x)}{v_b} \quad (C = \text{const.}), \qquad (10)$$

where $I_b(x)$ is the beam intensity and v_b the beam velocity, formula (9) can be modified as follows,

$$\frac{\frac{1}{N_{\nu A}^{fl}(x)} \frac{dN_{\nu A}^{fl}(x)}{dx}}{\frac{1}{N_{\nu B}^{fl}(x)} \frac{dN_{\nu B}^{fl}(x)}{dx}} = \frac{\frac{\langle \sigma_i^A v \rangle}{v_A}}{\frac{\langle \sigma_i^B v \rangle}{v_B}} = g(T_e(x)) \qquad (11)$$

Therefore we can obtain the local electron temperature $T_e(x)$ from the value of the ratio of two effective cross sections for electron impact ionization, which is equal to the measured value of the ratio of the attenuations of two beams.

3. Selection of Probing Beam Species

3.1 n_e measurement

We may use a neutral Li-beam for this purpose for the following reasons:

(i) The cross section for electron impact excitation, σ_{ex}, is accurately known /11/, and $\langle \sigma_{ex} v \rangle$ is very large and insensitive to T_e. The change of $\langle \sigma_{ex} v \rangle$ is of 10 % at most in the range of 10 eV to 100 eV (see Fig. 1).

(ii) A tunable dye laser (670.8 nm) for pumping is available. Because of the two level system it is easy to get the saturation condition which results in a simple data analysis. In addition to that, only the relative measurements of N_{ν}^{ex} and N_{ν}^{fl} are required because they are observed at the same wavelength (resonance line of Li I, 670.8 nm).

(iii) The contamination of the plasma by impurity injection is reduced due to the low-Z impurity (Z = 3).

3.2 T_e measurement

The following characteristics are required for species of two probing neutral beams which are used for this diagnostics:

(i) The cross sections for electron impact ionization are known. One of the effective cross sections is sensitive to T_e and the other is insensitive to T_e.

(ii) They attenuate suitably in the boundary layer,

$$\int n_e(x) \frac{\langle \sigma_i v \rangle}{v_b} dx \sim 1 \text{ for } x \sim 5 \text{ cm}.$$

(iii) Tunable dye lasers for pumping are available.

The characteristics for the matters mentioned above are tabulated for various species in Table 1.
We may use Al or Ti as species where the ionization rate coefficien $\langle \sigma_i v \rangle$ is sensitive to T_e below 100 eV and Li for an insensitive rate coefficient /12 - 15/ (see Fig. 1). Generally a species of whi the ionization rate coefficient is sensitive to T_e, needs a short wavelength laser for pumping which is not easily available.

For Al and Ti, the ionization rate coefficients are moderately sensitive to T_e and the tunable dye lasers for pumping them are available with the technique of frequency doubling. It is straightforward to use Li as a species being insensitive to T_e, since we plan to measure n_e and T_e simultaneously with one apparatus. It is also possible to use Na instead of Li because the resonance excitation cross section for Na by electron impact is also well known /16/. For the pumping of Na, however, an attention should be payed to the existence of two resonance transitions of 589.0 nm and 589.6 nm in the case of the n_e measurement (in the range of anomalous Zeeman effect at 3o kG still). The ratios between two effective cross sections for electron impact ionization, $g(T_e)$, are shown for Li-Al and Li-Ti as a function of T_e in Fig. 2. The energy of the atomic beam injected into the plasma is assumed to be 5 eV. In Fig. 2, we see that $g(T_e)$ for both cases are reasonably sensitive to T_e between 1 eV and 100 eV.

4. Production of Probing Beams

The mean free paths, λ, for the neutral beams of Li, Al and Ti in a plasma of $n_e = 10^{12}\ cm^{-3}$ and $T_e = 10$ eV are shown as a function of beam energy in Fig. 3. Their mean free paths at energies of several eV become 2 - 2o cm, which is in the order of the length of the scrape-off layer in tokamaks. A beam of several eV energy can be produced by means of LIE. An Al beam with the density of $10^{11}\ cm^{-3}$ at 14o cm from the source and a near Maxwellian velocity distribution of the peak energy of 5 eV was produced by vapourizing thin Al films (2 μm) coated on a glass plate by the shooting of a Nd-YAG laser (7 J/cm^2, 4o ns) from the back of the glass plate /5/. Such a beam can also be used as the probing beam for active diagnostics.
Two beams for the T_e measurement may be produced by shooting a ruby laser (or Nd-YAG laser etc.) onto a two component target. The two component target can be made by two layer coatings of Li and Al (or Ti) on a glass plate or a compound species (for instance Li-Al). For the former, the coating of Al on the Li layer also plays a role preventing air exposure of Li, because Li atoms are chemically very reactive. The beam density and energy can be controlled by changing the target thickness and the laser power.

5. Accuracy of the Method

The error of the n_e measurement arises from the inaccuracy of $\langle \sigma_{ex} v \rangle$, V_1/V_b and N_ν^{ex}/N_ν^{fl}, since the remaining quantities in formula (7) are accurately known. The resonance excitation cross section σ_{ex} for Li by electron impact has been determined within an error of 5 % /11/. In addition to that, however, the ambiguity of $\langle \sigma_{ex} v \rangle$ by the change of T_e should be considered, which is estimated to be about 5 %. For the measurement of V_1/V_b, it may be reasonable to estimate that the ambiguity for the determination of the diameter of each beam is of about 5 %. In this case, it is assumed that the image of the entrance slit of the optical detection system is in the crossing region of the two beams.

For the measurement of N_ν^{ex}/N_ν^{fl}, firstly we must consider the Zeeman effect of the related transition in the application to a plasma confined by magnetic fields. For a tokamak with the toroidal magnetic field above 1o kG, we see three Zeeman components (normal triplet) by Paschen-Back effect for the Li resonance line in the case of the observation perpendicular to the magnetic field which is the normal situation in tokamak experiments. The emission N_ν^{ex} produced by electron impact excitation should be measured by an optical detection system which has the spectral width covering all the Zeeman components so that the ambiguity caused by the polarization of the emission is eliminated. The population of the upper sub-levels which cause the emission N_ν^{fl} depends on the polarization of the pumping dye laser light, while the sub-levels are equally populated in the case of N_ν^{ex} produced by isotropical electron impact excitation. There are two procedures to measure N_ν^{fl}. One of them is to pump all the Zeeman components by using the unpolarized dye laser light or polarized light which has both polarization components parallel and perpendicular to the magnetic field. The other is to pump only the π component by using the dye laser light with the polarization parallel to the magnetic field and a narrow spectral width. In the latter case if collision effects among the sub-levels can be neglected, the values of $g_1 = 2$ and $g_2 = 2$ should be used in formula (7) because the sub-levels of the azimuthal quantum number $m_1 = 0$ are only excited (on the other hand, $g_1 = 2$ and $g_2 = 6$ in the former case). Besides, the degree of anisotropy of N_ν^{fl} for the latter differs from that of N_ν^{ex}. The use of the unpolarized dye laser light reduces the ambiguity. Secondly, the dye laser spectra consist of many discrete longitudinal modes of which the separation is determined by the length of the laser cavity. This problem can be solved by using a high intensity dye laser because the dye laser has the effect of a continuous spectrum by the power broadening. In case of the Li resonance line (67o.8 nm) and the cavity length of 1 m it can be satisfied within the error of 1o % with the dye laser of the intensity of saturation parameters S ~ 16o (laser power of 4.4 kW/cm^2 Å)/17/. If the considerations mentioned above are carried out carefully, the value of N_ν^{ex}/N_ν^{fl} may be measured within the error of 10 %. Therefore n_e can be determined within an error of about 3o %.

In the case of the T_e measurement, there is no restriction related to the Zeeman effect, the polarization of the dye laser light and the saturation condition of the pumping, because the linear relation between N_ν^{fl} and I_b is only the necessary condition as seen from formulae (1o) and (11). A problem is that the distribution of the populations among the sub-levels of the ground state for Al (or Ti) might change at each radial position due to the different plasma parameters. This might cause an error, because the lowest sub-level is only used for pumping. We estimate, however, that the rearrangement of the population by collisional effects can be neglected for the boundary layer plasma ($n_e < 1o^{13}$ cm^{-3}) /10/. The main source of the error is the accuracy of the cross sections for electron impact ionization which strongly affects that of the T_e measurement. After evaluating the data of the ionization cross sections related to this method /12 - 15, 18 - 21/, the error for the determination of T_e is estimated to be 1o % below 2o eV and 4o % at 5o eV (see Appendix).

6. Application to TEXTOR Tokamak

Figure 4 shows the radial profile of the expected photon flux N_{ν}^{ex}, which is produced by electron impact excitation of the Li atoms injected at the beam energy of 5 eV and the incident beam density of 1×10^{9} cm^{-3}, in the scrape-off layer of TEXTOR. We assume $n_e = 5 \times 10^{12}$ cm^{-3} and $T_e = 30$ eV at the limiter position (r = 5o cm) and an exponential decay with an e-folding length of 2 cm. The results in WEGA /22/, ASDEX /23/, PDX and PLT tokamaks /24/ are taken into account for this assumption. Since a photon flux of 10^{15} cm^{-3} sec^{-1} is easily observable, a beam density of 10^{9} cm^{-3} is high enough for this measurement. Therefore, if these densities are achieved, the total amount of impurities injected is only about 10^{12} particles/pulse, which is about a factor of 10^{4} smaller than those in impurity injection experiments /3,4,25/. With this density it is expected that there is no problem for the contamination and the perturbation of plasmas. Figure 5 shows the behaviour of the attenuations for the Li-, Al- and Ti-atom beams of 5 eV in the scrape-off layer of TEXTOR. The assumption of the plasma parameters is the same as that in Fig. 4. We see that species of 5 eV are suitable for the observation of the beam attenuation.

The schematic diagram of the experimental set-up for TEXTOR is shown in Fig. 6. Two neutral beams can be produced by shooting a ruby laser from the back of a two component thin target. The two beams may arrive at the scrape-off layer at different times due to the different masses. Two tunable dye lasers for pumping them, will therefore be shot with a delay relative to the ruby laser. The photon signals can be measured with a multichannel detector which is position sensitive. Then, we can determine $n_e(r)$ and $T_e(r)$ with one shot of each laser. The transmission and the reflectance of the mirrors M_1 and M_2 should be determined suitably according to the species of two probing beams and the powers of two dye lasers.

The time sequence of the ruby laser and two dye lasers and the expected photon signals are shown in Fig. 7. It is assumed that the temperature of the two beams, T_b, is 5 eV and the distance between the target and the observation region, l, is 6o cm. In the case of a stationary source (hydrodynamic velocity $u \ll$ thermal velocity v_p) of atoms with a Maxwellian velocity distribution, the time-of-flight signal of the atoms at the distance l from the target is given by the following formula /26/:

$$S^{ex}(\tau) = \tau^{-4} \exp(-\tau^{-2}), \qquad \tau = \frac{t}{l} v_p = \frac{t}{l}\sqrt{\frac{2kT_b}{M}} \tag{12}$$

where t is the real time, v_p the peak velocity of the Maxwellian velocity distribution and M the atomic mass of the beam. In the case of a source moving with an hydrodynamic velocity $u > v_p$, the time width of the response of S^{ex} will be considerably reduced compared to the case of $u \approx 0$. Here, we consider the case of the stationary source. The signal for electron impact excitation of Li, S^{ex}, rises at about 2o μs after shooting the ruby laser, has a maximum at 35 μs and then gradually decreases. The sampling interval of 1o μs is limited by the dead time of the charge sensitive ADC of CAMAC. Since S^{fl} for Li is expected to be almost flat during the dye laser duration ($\sim$ 5oo ns) for the two level case, it can be measured with the sampling time $\Delta t \sim$ 1oo ns during this condition. The expected signal S^{ex} at r = 53 cm ($n_e \sim 1 \times 10^{12}$ cm^{-3}, $T_e \sim 7$ eV) is the following:

$$S^{ex} = N_\nu^{ex} V_b \frac{\Omega}{4\pi} \eta_t \eta_q \Delta t \sim 100 \quad [\text{Photoelectrons}] \tag{13}$$

where V_b (~ 1 cm^3) is the observation volume, Ω ($\sim 10^{-2}$) the solid angle, η_t ($\sim$ o.1) the transmission of the optical system, and η_q ($\sim$ o.o2) the quantum yield of the photomultiplier. The signal-to-noise ratio $S/N = \sqrt{S^{ex}}$ is 1o. The ratio of the expected signals, S^{ex}/S^{fl}, is about 1/8 at r = 53 cm from formula (7), as $g_1 = 2$, $g_2 = 6$, $A_{21} = 3{,}72 \times 10^7$ sec^{-1}, $\langle \sigma_{ex} v \rangle = 6.3 \times 10^{-7}$ cm^{3}sec^{-1} and $V_1/V_b \sim 1/5$. It is assumed that the diameters of the atomic beam and dye laser beam are 5 cm$^\phi$ and 1 cm$^\phi$, respectively, the magnification of the optical system is unity, the diameter of the optical fibers is o.5 cm$^\phi$, the spacing is 1 cm from each other, and all the Zeeman effect components are pumped by the dye laser. This arrangement gives a radial resolution Δr of o.5 cm for the n_e measurement and 1 cm for the T_e measurement. The ratio S^{ex}/S^{fl} can be controlled by changing the size of both beams.

The cross section for electron impact excitation of Al is smaller by a factor of 1o - 1o^2 than that of Li (also for Ti probably) /27/. As demonstration, the time behaviour of S^{ex} for Al and Ti, in which their total fluxes become roughly the same as that for Li, is shown in Fig. 7. The ratio of S^{fl} for Al (or Ti) to that for Li depends on the characteristics of the mirror M_2, η_t and η_q for the related wavelengths. This ratio can be made to be in the order of 1 by controlling the characteristics of M_2. The peak value of S^{fl} can be used in the case of Ti which is of the three level system, since the relative spatial profile of N_ν^{fl} is only necessary as mentioned before. The beam velocity necessary for calculation of the effective ionization cross sections can be exactly obtained from the time interval between the ruby laser and the dye laser. The distribution of the beam velocity in the range of the scrape-off layer ($\sim$ 5 cm) at the shooting time of the dye laser, Δv_b, is 1.3 x 1o^5 cm/sec for Li and 6.3 x 1o^4 cm/sec for Al. The densities of the atomic beams within these velocity distributions are almost constant without a plasma. The change of Doppler shift due to it is o.oo3 nm for the Li resonance line (67o.8 nm) which is the laser spectral width necessary for simultaneous excitation of all atoms in the scrape-off layer. The Zeeman splitting, $\Delta\lambda_Z$, at 2o kG is o.o42 nm (whole spectral width $2\,\Delta\lambda_Z$ = o.o84 nm) for 67o.8 nm of Li atoms. Therefore the laser spectral width of o.15 nm is wide enough and this width leads to a dye laser power of 6.6 kW/cm^2 to get S = 16o. Though it is assumed that the energies of two beams are equal, this assumption is not essential for this method. Even if their energies are not equal, their intensities can be adjusted by delaying the shooting time of the dye laser.

The background from the tokamak plasma in the visible and UV region arises from free-free and free-bound continuum and line radiation (mainly HI, OII and OIII). The continuum radiation from a tokamak plasma of $\bar{n}_e \sim 2 \times 10^{13}\,cm^{-3}$ is neglegibly small compared to N_ν^{ex} and N_ν^{fl}, when the observation is done at a chord height far from the plasma center as seen in /28/. Using filters

($\Delta\lambda \sim$ 3nm), some impurity lines (OII:444.3 nm $\sim$ 446.9 nm and 672.1 nm) might appear. In the case of Ti, however, the density of 1.7 x 10^8 cm^{-3} has successfully been measured with a constant background in the ASDEX tokamak /8/. Therefore we expect that the Li resonance line of 670.8 nm may also be measured with a background which is almost constant. Furthermore, in the measurements of N_ν^{fl} for Li and Al, the elimiation of the stray light caused by the pumping dye lasers is important because of the two level system. The density measurement of the order of 10^8 cm^{-3} should be possible by preparing careful apparatus arrangements (beam dump, view dump and so on).

5. Concluding Remarks

From the considerations mentioned above, space- and time-resolved measurements of the plasma parameters, n_e (r,t) and T_e (r,t), in the boundary layer of tokamaks with this method seem to be possible. The beams of the incident atom density of about 10^9 cm^{-3} and the energy of about 5 eV are necessary for the application to tokamaks. This method does not disturb plasmas so much and is also applicable for diagnostics of plasmas of $n_e \lesssim 10^{13}$ cm^{-3}, $T_e \lesssim 100$ eV and the plasma size $\sim$ 5 cm. For the more accurate determination of T_e, the measurements of the partial cross sections σ_i^{Z+} (see Appendix) for electron impact ionization of Al and Ti are desired. Since first walls consisting of TiC (or TiN etc.) might be used in future tokamaks, there might also be a possibility of "in situ" measurements using the first wall as two component target.

Acknowledgements

We would like to thank Prof. H.-J. Kunze and Dr. F.J. de Heer for helpful discussions on atomic processes. We also wish to thank Drs. Y.T. Lie, B. Schweer, E. Dullni and Ph. Mertens for useful advices on laser-induced fluorescence.

Appendix: Cross Sections for Electron Impact Ionization

Figure 8 shows the comparison between the ionization rate coefficients calculated with the data of the experimental cross sections /12 - 14/ and the semi-empirical formula of Lotz /18/ for Li and Al. For Li, Lotz /19/ used the experimental data of McFarland and Kinney /2o/ to evaluate the cross section. The data of McFarland and Kinney are larger by a factor of 2 than those of the Born approximation in the energy region from 1oo to 6oo eV where the measurement was carried out. Jalin et al. /13/ experimentally obtained the results which agree well with the Born approximation above 2oo eV. They pointed out that the discrepancy between both experiments is considered mainly due to the ambiguity of the measurement of the Li-atom density by means of surface ionization which was used by McFarland and Kinney (Jalin et al. used the deposition method). We use the effective ionization cross section for Li which is calculated with the cross section data of Zapesochnyi and Aleksakhin /12/ at lower energy (data, threshold - 3o eV) and Jalin et al. at higher energy (data, 1oo eV - 2ooo eV). The use of their cross sections has also been recommended by Bell et al. /29/.
For Al the discrepancy between the rate coefficients calculated with the experimental cross section data of Shimon et al./14/ and the semi-empirical formula of Lotz /18/ is considerably large at higher temperature. Zapesochnyi et al. /2o/ pointed out that double ionization under conditions of single collisions is effective for the Al group elements, while it was not considered in Lotz's evaluation /18/. Therefore we use the effective cross section calculated with the experimental data, as the discrepancy is mainly due to double ionization. Since the experimental cross section, however, is a total one ($\sigma_i = \sum_Z Z\,\sigma_i^{Z+}$, Z: charge state), the use of the total cross section, for which the contribution from double ionization is not small, overestimates the beam attenuation. The effective ionization cross section ($\sigma_{eff} = \langle \sum_Z \sigma_i^{Z+} v \rangle / v_b$) which is related to the beam attenuation may be in the middle of the region between the experiment and the semi-empirical formula of Lotz. The comparison between the experimental cross section by Shimon et al. and Lotz's cross section is shown in Fig. 9. If it is assumed that the difference

between the experimental cross section and Lotz's cross section normalized to the experimental one should be the cross section for double ionization, the dotted curve corresponds to the sum of the partial ionization cross sections ($\sum_Z \sigma_i^{Z+}$). The ratio,g, between the effective ionization cross section for Li and that calculated with the cross section $\sum_Z \sigma_i^{Z+}$ for Al is also shown with the dashed curve for comparison in Fig. 2.
For Ti, we can find no available experimental data and use Lotz's formula /15/. From Fig. 2 the uncertainty of the cross section data might cause errors of 1o % for the determination of T_e below 2o eV and 4o % at 5o eV, as the ambiguity for Al (or Ti) is dominant.

References

/1/ K. Kadota, K. Tsuchida, Y. Kawasumi and J. Fujita, Plasma Physics 2o (1978) 1o11

/2/ K. Kadota, K. Matsunaga, H. Iguchi, M. Fujiwara, K. Tsuchida and J. Fujita, Jpn. J. Appl. Phys. 21 (1982) L 26o

/3/ E.S. Marmar, J.L. Cecchi and S.A. Cohen, Rev. Sci. Instrum. 46 (1975) 1149

/4/ T. Yamauchi, M. Nagami and S. Sengoku, Jpn. J. Appl. Physics 19 (198o) 1737

/5/ C. Breton, C. de Michelis, W. Hecq and M. Mattioli, Revue Phys. Appl. 15 (198o) 1193

/6/ P. Bogen and E. Hintz, Comments on Plasma Phys. Cont. Fusion 4 (1978) 115

/7/ E. Hintz, J.Nucl. Mat. 93/94 (198o) 86

/8/ E. Dullni, P. Bogen, E. Hintz, D. Rusbüldt, B. Schweer, S. Goto and K.H. Steuer, Phys. Letters 88 A (1982) 4o

/9/ E. Dullni, (1982) private communication

/1o/ H.C. Meng and H.-J. Kunze, Phys. Fluids, 22 (1979) 1o82

/11/ D. Leep and A. Gallagher, Phys. Rev. A 1o (1974) 1o82

/12/ I.P. Zapesochnyi and I.S. Aleksakhin, Sov. Phys. JETP 28 (1969) 41

/13/ R. Jalin, R. Hagemann and R. Botter, J. Chem. Phys. 59 (1973) 952

/14/ L.L. Shimon, E.I. Nepiipov and I.P.Zapesochnyi, Sov. Phys. Tech. Phys. 2o (1975) 434

/15/ W. Lotz, Z. Phys. 22o (1969) 466

/16/ E. A. Enemark and A. Gallagher, Phys. Rev. A 6 (1972) 192

/17/ E. Hintz, D. Rusbüldt, B. Schweer, J. Bohdansky, J. Roth and A.P. Martinelli, J. Nucl. Mat. 93/94 (198o) 656

/18/ W. Lotz, Z. Phys. 216 (1968) 241

/19/ W. Lotz, Astrophys. J. Suppl. 14 (1967) 2o7

/2o/ R.H. McFarland and J.D. Kinney, Phys. Rev. 137 (1965) A1o58

/21/ I.P. Zapesochnyi, J.E. Kontros and L.L. Shimon, Abstracts of the 9 th Int. Conf. on the Physics of Electronic and Atomic Collisions, Seattle (1975) 9oo

/22/ G. Ichtchenko, report EUR-CEA-FC-1o41, Fontenay-aux Roses (198o)

/23/ ASDEX-team, Proc. IAEA Technical Committee Meeting on Divertors and Impurity Control (1981) 23

/24/ R. Budny, report PPPL-1876, Plasma Physics Lab., Princeton University (1982)

/25/ TFR-Group, Phys. Letters 87 A (1982) 169

/26/ C. Peugnet, J. Appl. Phys. 48 (1977) 32o6

/27/ R.K. Peterkop and Yu. I. Ryabykh, Opt. Spectrosc. (USSR) (Engl. Translation) 45 (1979) 111

/28/ K.Kadota, M. Otsuka and J. Fujita
Nucl. Fusion 2o (198o) 2o9

/29/ K.L. Bell, H.B. Gilbody, J.G. Hughes, A.E. Kingston and F. J. Smith
Report CLM-R216, Culham (1982)

Table 1: Characteristics of various atoms

Species	Z	Wavelength for pumping	Wavelength for observation	Ionization cross section	T_e dependence on ionization rate	Mean free path+
Li	3	67o.8 nm (^2S-$^2P^o$)	67o.8 nm	Exp.	Insensitive	19 cm
Be	4	234.9 (^1S-$^1P^o$)	234.9	Semi-emp.	Sensitive	34
B	5	249.7 ($^2P^o$-^2S)	249.7,249.8	"	"	33
C	6	156.1 (^3P-$^3D^o$)	156.o,156.1	Exp.	"	5o
Na	11	589.o 589.6 (^2S-$^2P^o$)	589.o 589.6	"	Insensitive	7.2
Mg	12	285.2 (^1S-$^1P^o$)	285.2	"	Sensitive	1o
Al	13	3o8.2 ($^2P^o$-^2D)	3o8.2,3o9.3	"	"	7.8
Si	14	251.4 (^3P-$^3P^o$)	251.4,251.9 252.9	Semi-emp.	"	8.6
Ti	25	294.2 (a^3F-v^3F^o)	445.3 (b^3F-v^3F^o)	"	"	3.8
Fe	26	3o2.1 (a^5D-y^5D^o)	382.o (a^5F-y^5D^o)	"	"	4.6

+The mean free path under conditions of the probing beam energy E_b = 5 eV, n_e = $1o^{12}$ cm^{-3} and T_e = 1o eV.

Figure Captions

Fig. 1 Rate coefficients for electron impact excitation and ionization. Li + e(exc) calculated with the data of Ref. 11, Li + e (ion), Refs. 12 and 13, Al + e (ion.) Ref.14 and Ti + e (ion.) Ref. 15.

Fig. 2 Ratios between two effective cross sections for electron impact ionization as a function of electron temperature. See Appendix for the dashed curve on Li-Al.

Fig.3 Mean free paths of various neutral beams in the plasma of $n_e = 10^{12}$ cm^{-3} and T_e = 10 eV as a function of beam energy.

Fig. 4 Expected radial profile of the photon flux, N_ν^{ex}, produced by electron impact excitation of the neutral Li-beam injected at energy of 5 eV into the scrape-off layer of TEXTOR. The incident Li-beam density $n_{Li}(a)$ is assumed to be 10^9 cm^{-3}.

Fig. 5 Expected radial profiles of the intensity of the neutral atoms injected at an energy of 5 eV into the scrape-off layer of TEXTOR.

Fig.6 Schematic experimental diagram for TEXTOR.

Fig. 7 Time sequence of a ruby laser for LIE and two dye lasers for LIF, and expected time behaviour of the signals for N_ν^{ex} and N_ν^{fl}.

Fig. 8 Comparison between experimental and semi-empirical rate coefficients for electron impact ionization.

Fig. 9 Comparison between experimental and semi-empirical cross-sections for electron impact ionization of Al.
——: exp. /14/, – – –: semi-emp. (Lotz) /18/,
—·—·: semi-emp. normalized to exp. and -----: sum of expected partial ionization cross sections ($\sum_Z \sigma_i^{Z+}$).

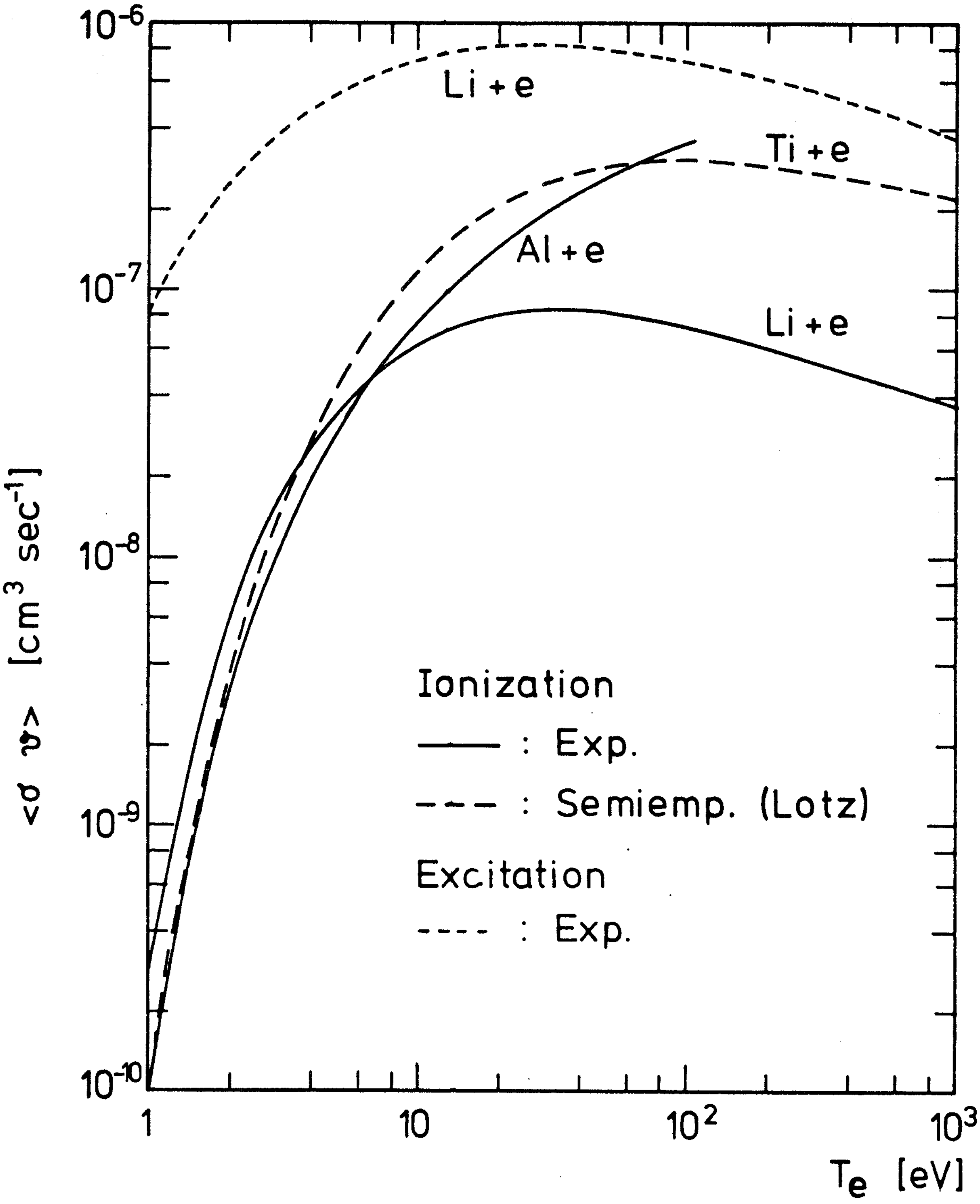

10^-6
10^-7
10^-8
10^-9
10^-10
<σ v> [cm^3 sec^-1]
1
10
10^2
10^3
T_e [eV]
Li + e
Ti + e
Al + e
Li + e
Ionization
: Exp.
: Semiemp. (Lotz)
Excitation
: Exp.

Fig. 1

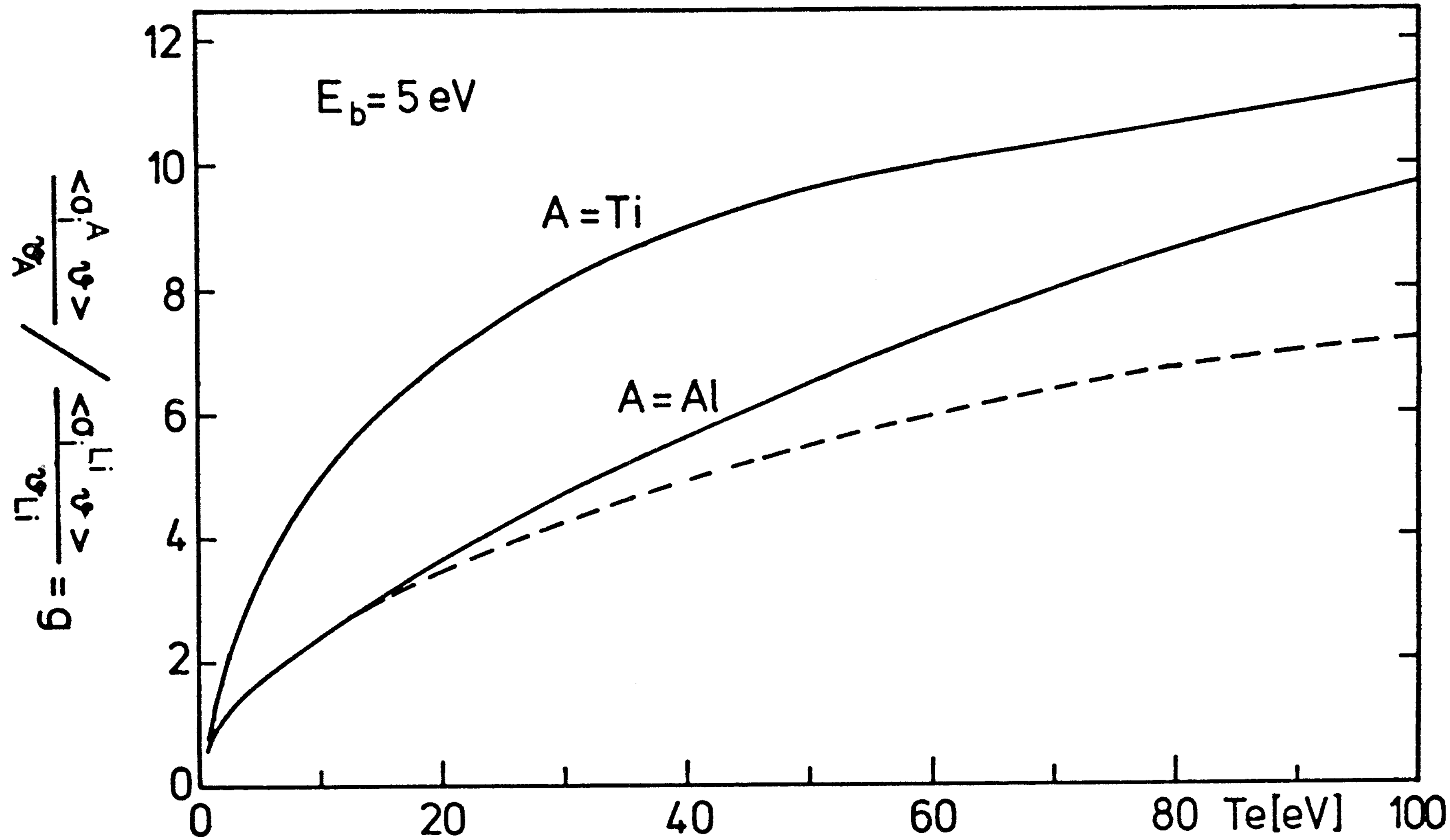

g = <σ_i^Li ϑ> / ϑ_Li / <σ_i^A ϑ> / ϑ_A
E_b = 5 eV
A = Ti
A = Al
0
2
4
6
8
10
12
0
20
40
60
80
100
Te[eV]

Fig. 2

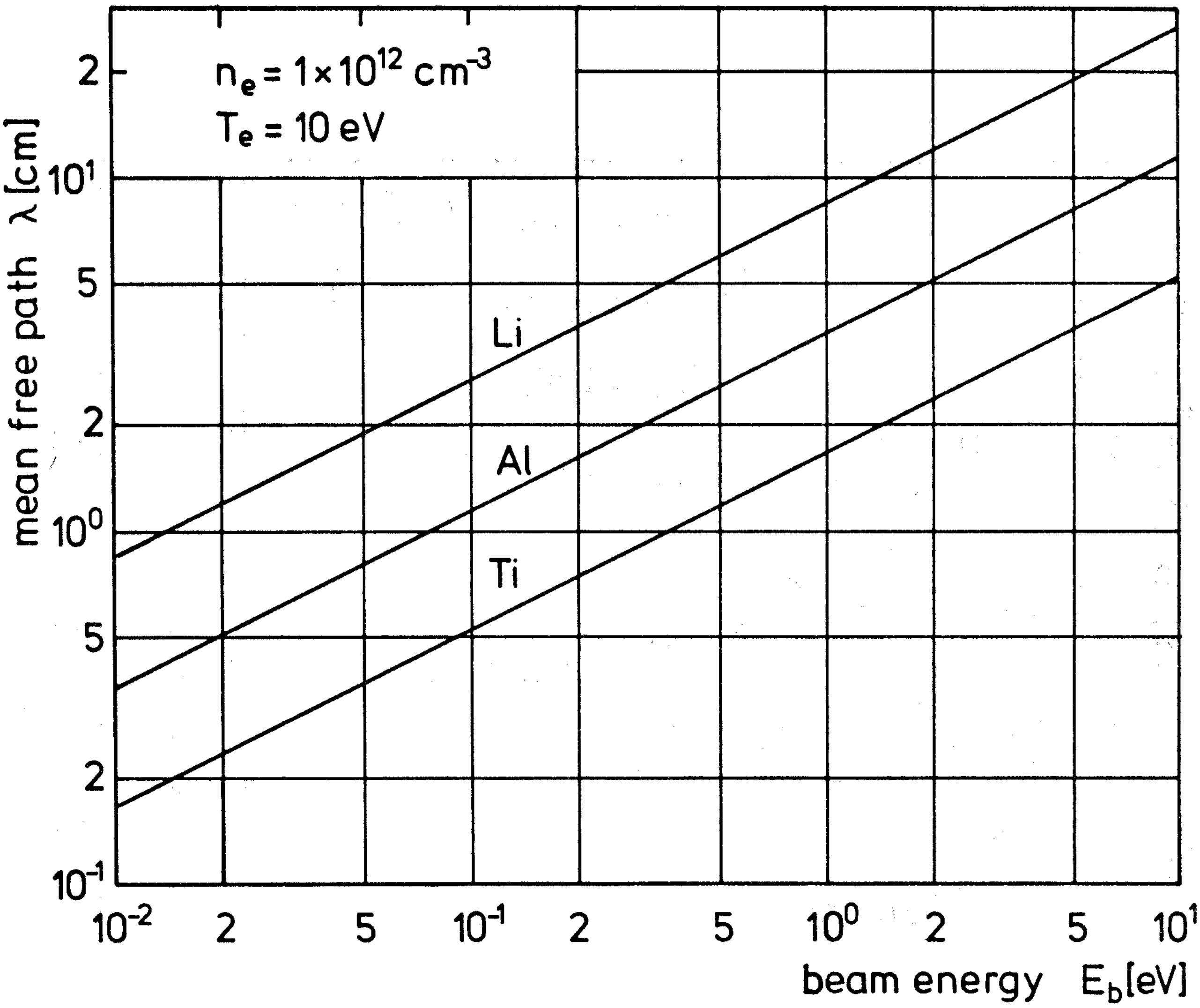

$n_e = 1 \times 10^{12}\ cm^{-3}$
$T_e = 10\ eV$
Li
Al
Ti
mean free path λ [cm]
10^{-1}
2
5
10^{0}
2
5
10^{1}
2
10^{-2}
2
5
10^{-1}
2
5
10^{0}
2
5
10^{1}
beam energy E_b[eV]

Fig. 3

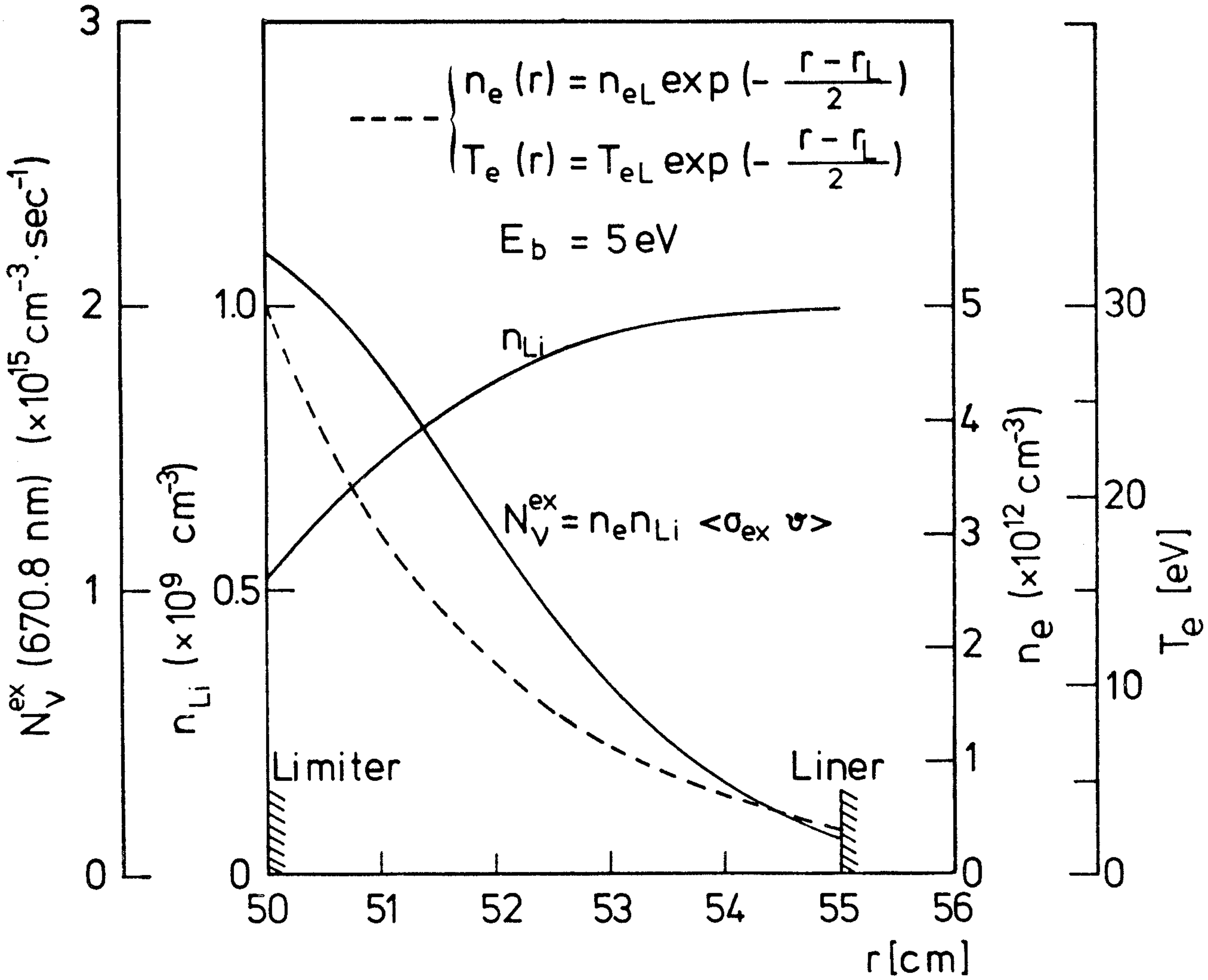

$n_e(r) = n_{eL} \exp(-\frac{r - r_L}{2})$
$T_e(r) = T_{eL} \exp(-\frac{r - r_L}{2})$
$E_b = 5\,eV$
n_{Li}
$N_V^{ex} = n_e n_{Li} \langle \sigma_{ex} v \rangle$
Limiter
Liner
N_V^{ex} (670.8 nm) ($\times 10^{15}\,cm^{-3}\cdot sec^{-1}$)
n_{Li} ($\times 10^9\,cm^{-3}$)
n_e ($\times 10^{12}\,cm^{-3}$)
T_e [eV]
r [cm]

Fig. 4

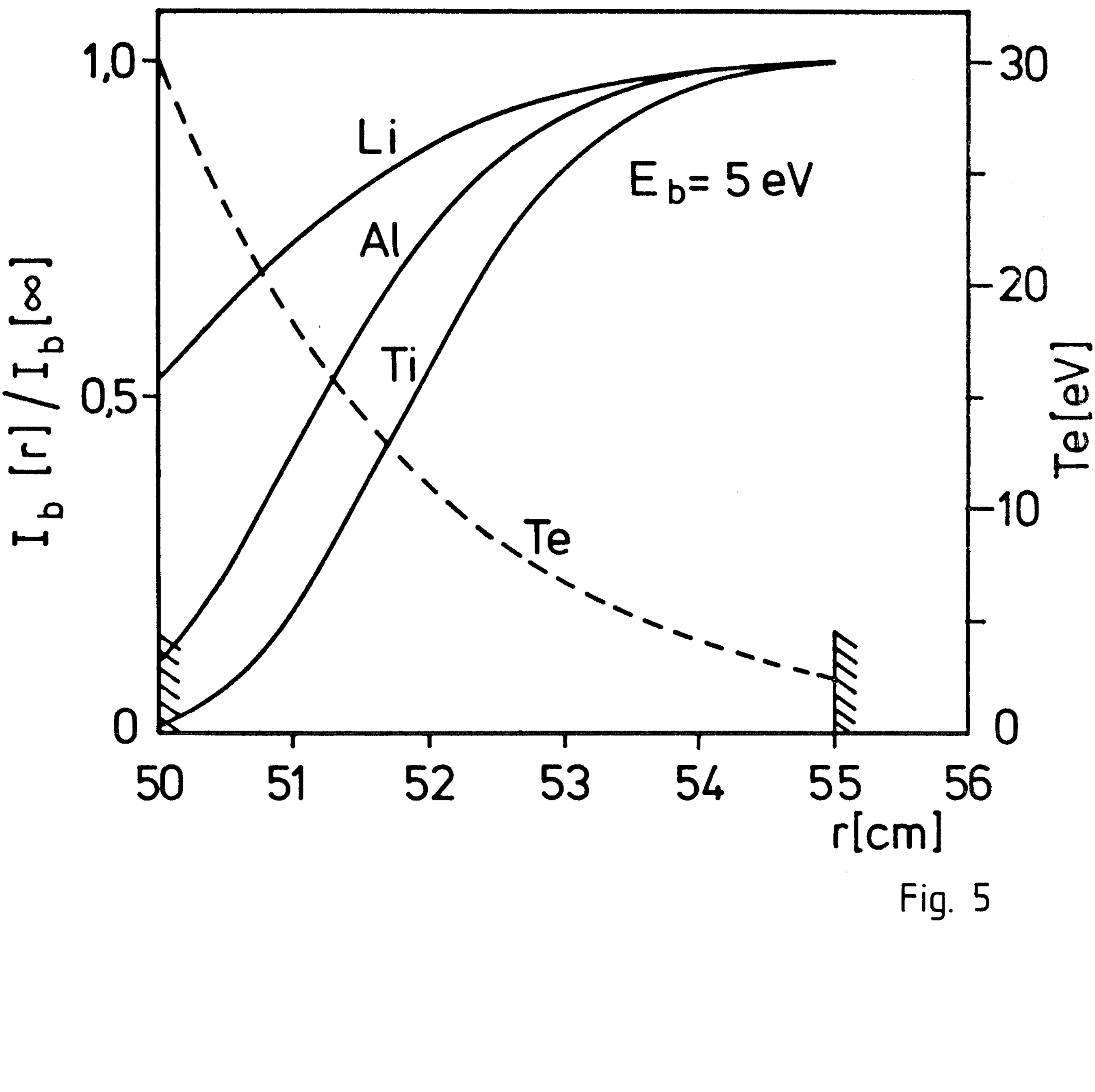

1,0
0,5
0
$I_b\,[r]\,/\,I_b\,[\infty]$
Li
Al
Ti
Te
$E_b = 5\ eV$
30
20
10
0
Te [eV]
50
51
52
53
54
55
56
r[cm]

Fig. 5

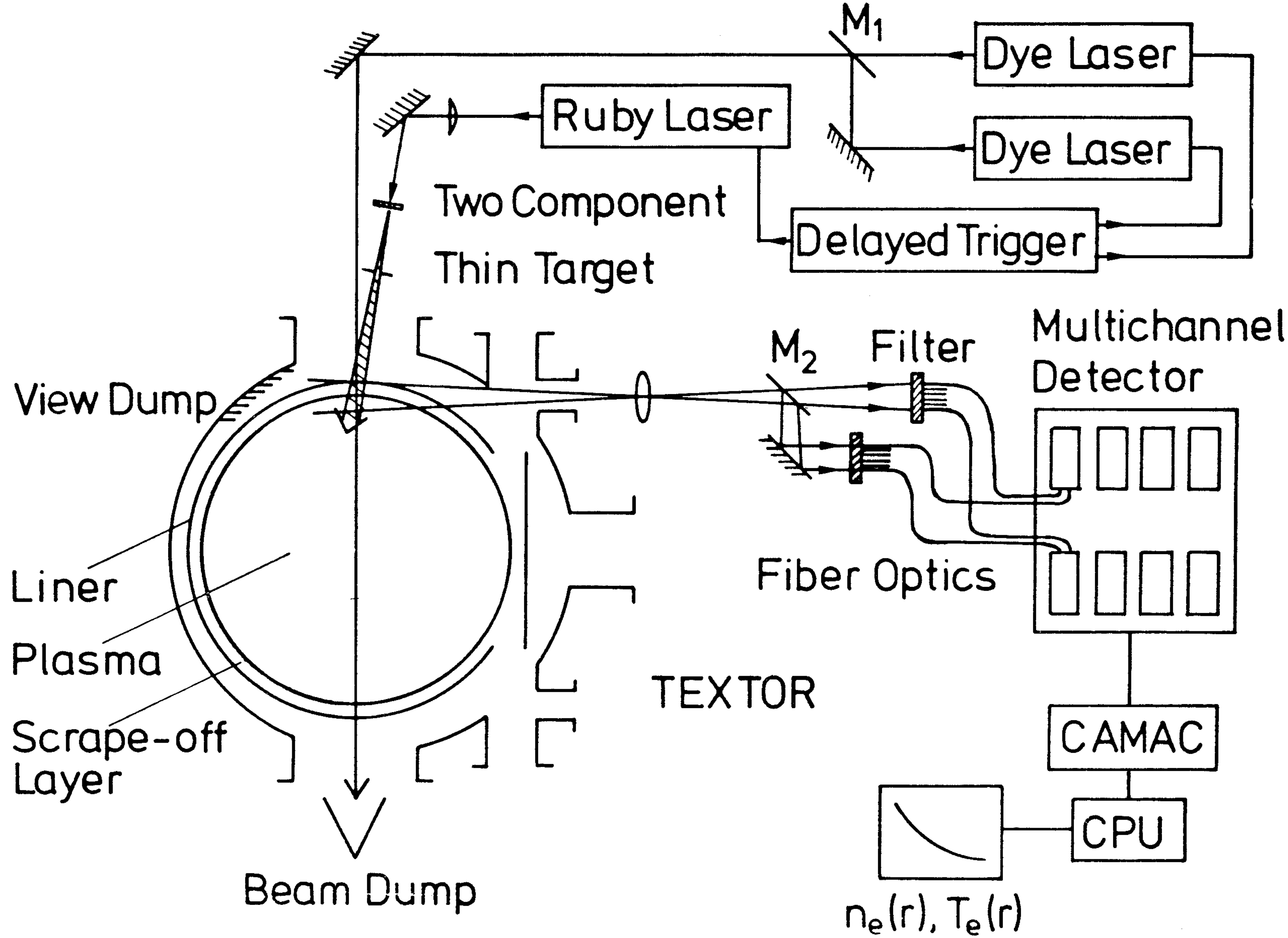

M1
Dye Laser
Dye Laser
Ruby Laser
Delayed Trigger
Two Component
Thin Target
View Dump
Liner
Plasma
Scrape-off
Layer
Beam Dump
TEXTOR
M2
Filter
Multichannel
Detector
Fiber Optics
CAMAC
CPU
$n_e(r)$, $T_e(r)$

Fig. 6

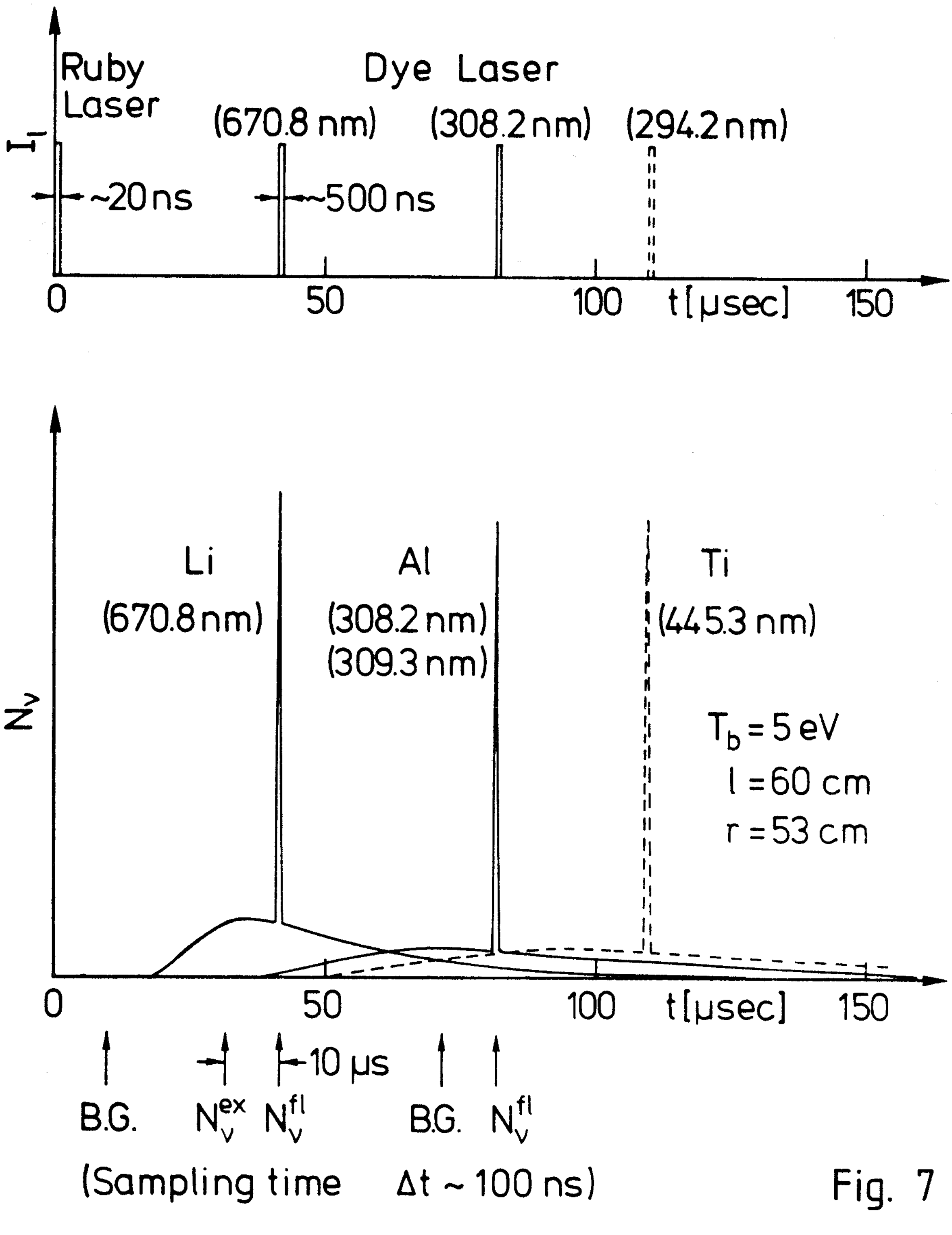
Ruby Laser
Dye Laser
(670.8 nm)
(308.2 nm)
(294.2 nm)
I_l
~20 ns
~500 ns
0
50
100
t [μsec]
150
Li
(670.8 nm)
Al
(308.2 nm)
(309.3 nm)
Ti
(445.3 nm)
$T_b = 5$ eV
$l = 60$ cm
$r = 53$ cm
N_ν
0
50
100
t [μsec]
150
10 μs
B.G.
N_ν^{ex}
N_ν^{fl}
B.G.
N_ν^{fl}
(Sampling time Δt ~ 100 ns)

Fig. 7

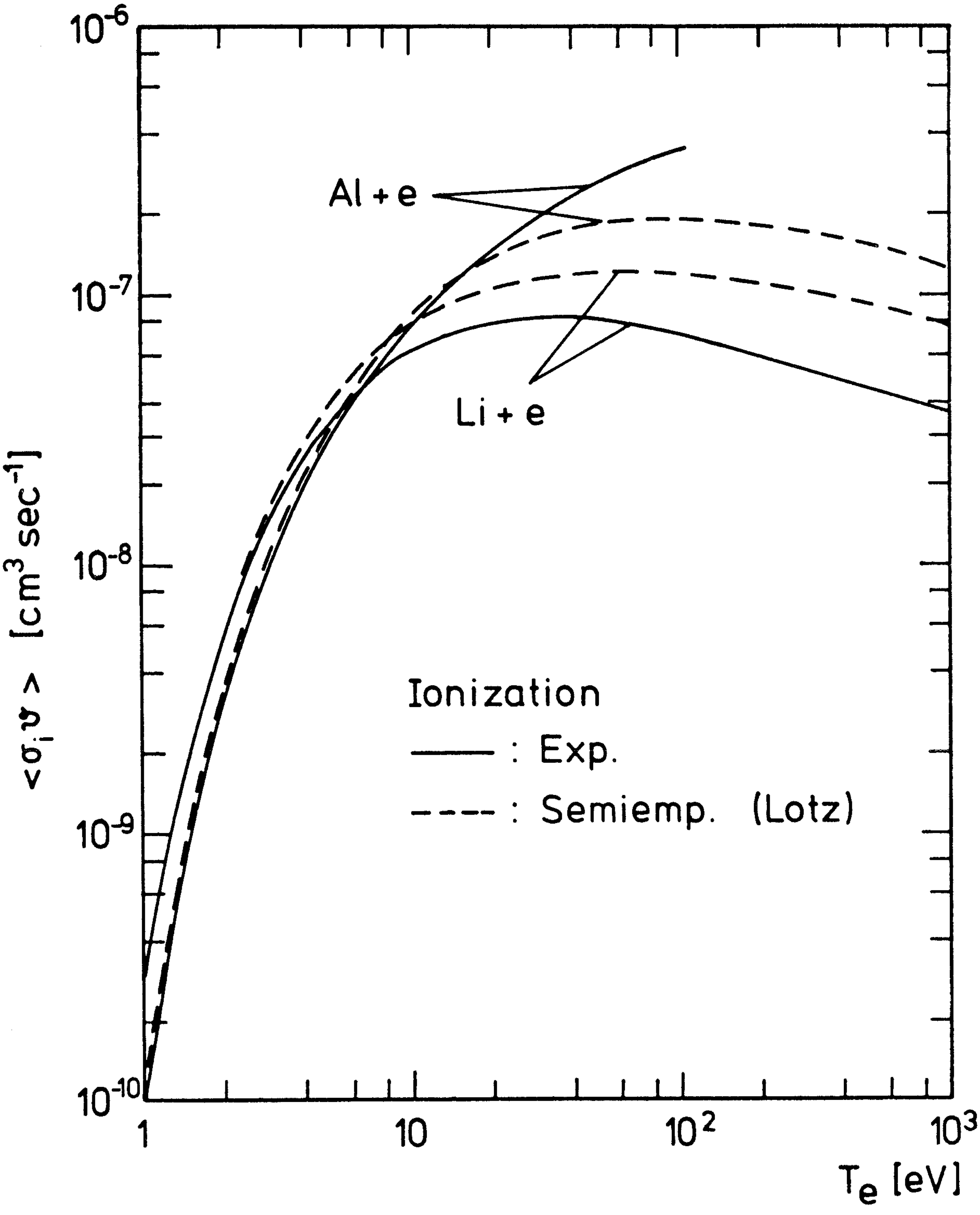

10^{-6}
10^{-7}
10^{-8}
10^{-9}
10^{-10}
1
10
10^2
10^3
T_e [eV]
$<\sigma_i v>$ [$cm^3 sec^{-1}$]
Al + e
Li + e
Ionization
: Exp.
: Semiemp. (Lotz)

Fig. 8

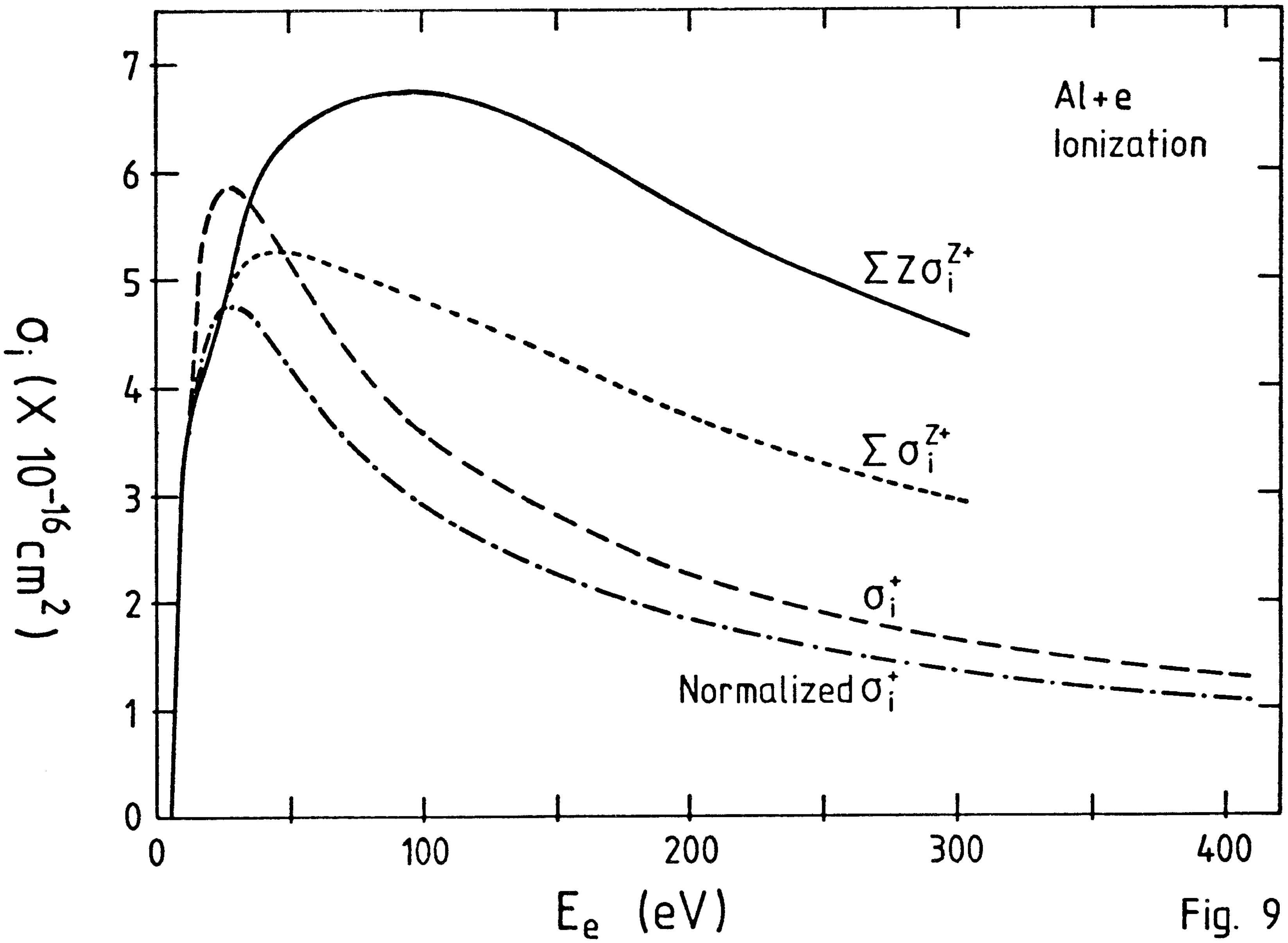
Al + e
Ionization
$\sum Z\sigma_i^{Z+}$
$\sum \sigma_i^{Z+}$
σ_i^{+}
Normalized σ_i^{+}
σ_i (X 10^{-16} cm^2)
0
1
2
3
4
5
6
7
0
100
200
300
400
E_e (eV)

Fig. 9